Modern radio engineering and telecommunication systems

Современные радиотехнические и телекоммуникационные системы

UDC 681.883.45
https://doi.org/10.32362/2500-316X-2023-11-1-31-40

RESEARCH ARTICLE

Hydroacoustic communication channel capacity

Valery E. Denisov @

MIREA – Russian Technological University, Moscow, 119454 Russia
@ Corresponding author, e-mail: denisov@mirea.ru

Abstract
Objectives. Capacity, describing the maximum rate of information transmission, is an important characteristic of any communication channel. The main purpose of this work is to determine the capacity of a hydroacoustic communication channel with constrained average intensity of the transmitted signal. An additional aim consists in finding the optimal spectrum of a transmitted signal and calculate its boundary frequencies. A model of a single-path channel was considered, which is characteristic of the deep sea with the receiver or transmitter placed at a sufficient depth.
Methods. Concepts of applied hydroacoustics, the theory of random processes, and information theory were used.
Results. An expression for gain in a hydroacoustic communication channel has been obtained. A novel expression derived for the spectral level of sea noise caused by sea surface waves is based on piecewise linear approximation of the curves of the spectral levels of noise obtained from four sources: turbulence, shipping, sea waves, and the thermal noise of the sea. Dependencies of the hydroacoustic channel capacity on communication distance, intensity of the transmitted signal, and sea state, are characterized. The definition of the optimal spectrum itself is determined along with the lower and upper boundary frequencies of the optimal spectrum of the transmitted signal. The dependence of the bandwidth usage on the intensity of the input signal at various communication distances has been investigated.
Conclusions. On the basis of the Francois–Garrison attenuation coefficient, channel capacity was correlated with the parameters of the marine environment: temperature, salinity, and pH in the study area. At a given intensity of the input signal, channel capacity was shown to decrease significantly with increasing distance and sea wave intensity. It is also shown that the width of the optimal spectrum decreases with increasing distance. Sea wave noise was noted to affect significantly the shape of the optimal spectrum and its boundary frequencies. The possibility of cases where bandwidth usage increases with increasing distance at a given input signal intensity cannot be ruled out.

Keywords: hydroacoustic communication channel, sea noise, spectral intensity of sea noise, signal intensity, bandwidth, optimal spectrum, channel bandwidth utilization

• **Submitted:** 28.04.2022 • **Revised:** 21.06.2022 • **Accepted:** 10.11.2022

For citation: Denisov V.E. Hydroacoustic communication channel capacity. *Russ. Technol. J*. 2023;11(1):31–40. https://doi.org/10.32362/2500-316X-2023-11-1-31-40

Financial disclosure: The author has no a financial or property interest in any material or method mentioned.

The author declares no conflicts of interest.

НАУЧНАЯ СТАТЬЯ

Пропускная способность гидроакустического канала связи

В.Е. Денисов @

МИРЭА – Российский технологический университет, Москва, 119454 Россия
@ *Автор для переписки, e-mail: denisov@mirea.ru*

Резюме
Цели. Пропускная способность является важной характеристикой любого канала связи, так как определяет предельную скорость передачи информации в нем. Основная цель работы – определение пропускной способности гидроакустического канала связи при ограничении на среднюю интенсивность передаваемого сигнала. Дополнительной задачей являлось определение оптимального спектра передаваемого сигнала и расчет граничных частот этого спектра. Была рассмотрена модель однолучевого канала, характерная для глубокого моря, когда приемник или передатчик расположены на достаточной глубине.
Методы. Использованы положения прикладной гидроакустики, теории случайных процессов и теории информации.
Результаты. Получено выражение для коэффициента передачи гидроакустического канала связи и новое выражение для спектрального уровня шумов моря, обусловленных волнением поверхности моря. На основе кусочно-линейной аппроксимации кривых спектральных уровней шумов турбулентности, судоходства, волнения моря и теплового шума моря определена спектральная плотность интенсивности шума моря. Получены зависимости пропускной способности гидроакустического канала от дальности связи, интенсивности передаваемого сигнала и состояния поверхности моря. Определены нижняя и верхняя частоты оптимального спектра передаваемого сигнала и оптимальный спектр. Исследована зависимость коэффициента использования полосы частот от интенсивности входного сигнала для разных значений дальности связи.
Выводы. Использование коэффициента затухания Франсуа – Гаррисона позволило связать пропускную способность канала с параметрами морской среды: температурой, соленостью, значением водородного показателя в исследуемом районе. При заданной интенсивности входного сигнала пропускная способность существенно уменьшается с ростом дальности и усилением волнения моря. Показано, что с ростом расстояния ширина оптимального спектра уменьшается. Отмечается значительное влияние шума от волнения моря на форму оптимального спектра и значения его граничных частот. Было установлено, что возможны случаи увеличения коэффициента использования полосы частот ростом дальности при заданной интенсивности входного сигнала.

Ключевые слова: гидроакустический канал связи, шумы моря, спектральная интенсивность шумов моря, интенсивность сигнала, пропускная способность, оптимальный спектр, коэффициент использования полосы частот канала

• **Поступила:** 28.04.2022 • **Доработана:** 21.06.2022 • **Принята к опубликованию:** 10.11.2022

Для цитирования: Денисов В.Е. Пропускная способность гидроакустического канала связи. *Russ. Technol. J.* 2023;11(1):31–40. https://doi.org/10.32362/2500-316X-2023-11-1-31-40

Прозрачность финансовой деятельности: Автор не имеет финансовой заинтересованности в представленных материалах или методах.

Автор заявляет об отсутствии конфликта интересов.

INTRODUCTION

When developing digital hydroacoustic communication systems, the capacity of a given hydroacoustic communication channel (HACC), representing the maximum rate of information transmission at a given sea noise and given constraints on the transmitted signal, is of particular interest. Given knowledge of HACC capacity, it is always possible to estimate the efficiency of the communication system under development. HACC capacity has been estimated by a number of national and international researchers under various conditions. Works [1–4] are particularly noteworthy among works in which capacity determination techniques are described. The closest approach to that taken the present work is the one given in Stojanovic's study [1], where the capacity of a single-path HACC was obtained using the frequency dependencies of the attenuation coefficient and sea noise. Assuming nonspherical spreading, as it should be in the case with a point source, the Urick attenuation coefficient [5], which is notionally independent of the parameters of the marine environment, was used. Here, the so-called practical spreading approach was used, in which the sound intensity taken as inversely proportional to the distance to the power of 1.5. However, as was noted [5], if the properties of the marine environment are insufficiently known, it is recommended to apply the spherical law instead. The HACC capacity was also calculated [1] using a special approximating formula for the spectral noise density [6], which gives somewhat overestimated values in comparison with the Urick curves [6]. However, Stojanovic [1] considered only the case of calm sea conditions. In the present work, the capacity of a single-path HACC was calculated using the frequency dependence of the attenuation coefficient described by the Francois–Garrison formula. Considered the most accurate at the present time, this formula is based around the parameters of the marine environment. In addition, a simple and illustrative piecewise linear approximation of the spectral level of sea noise was used. The dependence of the channel capacity on the intensity of sea surface waves was additionally investigated. Considering research carried out in recent years, the works [7–9] should be noted, in which various hydroacoustic communication systems were analyzed and their corresponding information transmission rates estimated.

1. HYDROACOUSTIC CHANNEL GAIN

In the emission of a harmonic signal, the instantaneous pressure $p(t, R)$ in a boundless homogeneous absorbing marine environment at distance R from a point source can be represented as follows [10–12]:

$$p(t,R) = \sqrt{2}P(R)\cos\left[\omega\left(t - \frac{R}{c}\right)\right], \quad (1)$$

where

$$P(R) = P_0 \frac{R_0}{R}\exp\left[-\alpha_e\left(R - R_0\right)\right] \quad (2)$$

is the root-mean-square pressure, Pa; $\omega = 2\pi f$ is the angular velocity of the source vibrations, rad/s; c = 1500 m/s is the speed of sound in seawater; R is distance, m; α_e is the attenuation coefficient in the marine environment, Np/m; P_0 is the root-mean-square pressure at reference distance R_0 (typically, R_0 = 1 m).

From expressions (1) and (2), the complex gain of the HACC can be expressed:

$$H(j\omega) = \frac{R_0}{R}\exp\left[-\alpha_e\left(R - R_0\right) - j\omega\frac{R}{c}\right] = \\ = H(\omega)\exp[j\vartheta(\omega)],$$

where $H(\omega)$ is the frequency response and $\upsilon(\omega)$ is the phase response. They are found as follows:

$$H(\omega) = \left|H(j\omega)\right| = \frac{R_0}{R}\exp\left[-\alpha_e\left(R - R_0\right)\right],\ \upsilon(\omega) = -\omega R/c.$$

In practice, the attenuation coefficient is typically expressed in dB/km, and the distance R is expressed in kilometers. Then, at R_0 = 1 m, the formula for the frequency response takes the form

$$H(f) = \frac{1}{R_{\text{km}} \cdot 10^3}\exp(-0.115\,\alpha R). \quad (3)$$

As follows from expression (3), at a given communication distance R, the properties of the frequency response are completely determined by the frequency response of the attenuation coefficient. Therefore, let us dwell in more detail on the attenuation coefficient of seawater. α has to be calculated using various semi-empirical formulas obtained on the basis of theoretical and experimental data. One of such formulas for calculating α is the Francois–Garrison formula [13, 14], which was derived by analyzing and generalizing the known results of measurements in the ocean, including measurements in the Arctic. The sound attenuation coefficient α in the frequency range from 200 Hz to 1 MHz to a depth of 5 km can be represented as follows [13, 14]:

$$\alpha = \alpha_1 + \alpha_2 + \alpha_3, \text{ dB/km},$$

where α_1 is the absorption coefficient due to ionic relaxation of boron compounds (borates), α_2 is the absorption coefficient due to ionic relaxation of magnesium sulfate ($MgSO_4$), and α_3 is the absorption coefficient due to the shear viscosity of fresh water and the structural relaxation of fresh water molecules. These quantities are expressed as follows:

$$\alpha_1 = \frac{A_1 P_1 f_1 f^2}{f_1^2 + f^2},\ \alpha_2 = \frac{A_2 P_2 f_2 f^2}{f_2^2 + f^2},\ \alpha_3 = A_3 P_3 f^2.$$

In the above formulas, the frequency f is expressed in kHz, and A_i (i = 1, 2, 3), P_i (i = 1, 2, 3), f_1, and f_2 are written as follows:

$$A_1 = \frac{8.86}{c} \cdot 10^{0.78\text{pH} - 5},\ (\text{dB/km})\cdot\text{kHz}^{-1};$$

$$P_1 = 1, f_1 = 2.8(S/35)^{0.5} \cdot 10^{4 - 1245/\Theta}, \text{ kHz};$$

$$A_2 = 21.44\frac{S}{c}(1+0.025T),\ (\text{dB/km})\cdot\text{kHz}^{-1};$$

$$P_2 = 1 - 1.37\cdot 10^{-4}z + 6.2\cdot 10^{-9}z^2;$$

$$f_2 = \frac{8.17\cdot 10^{8-1990/\Theta}}{1+0.0018(S-35)},\ \text{kHz};$$

$$P_3 = 1 - 3.83\cdot 10^{-5}z + 4.9\cdot 10^{-10}z^2;$$

$$A_3 = \begin{cases} 4.937\cdot 10^{-4} - 2.59\cdot 10^{-5}T + \\ + 9.11\cdot 10^{-7}T^2 - 1.50\cdot 10^{-8}T^3, \\ T \le 20°\text{C}, \\ \\ 3.964\cdot 10^{-4} - 1.146\cdot 10^{-5}T + \\ + 1.45\cdot 10^{-7}T^2 - 6.50\cdot 10^{-10}T^3, \\ T > 20°\text{C}, \end{cases} \quad (\text{dB/km})\cdot\text{kHz}^{-2}.$$

Here, c is the speed of sound in seawater, m/s, which is approximately calculated as follows:

$$c \approx 1412 + 3.21T + 1.19S + 0.0167z;$$

T is the water temperature, °C; $\Theta = 273 + T$ is the water temperature expressed in kelvins, K; S is salinity, ‰; z is depth, m; and pH is the pH of the water in the area of measurement α. The pH of the ocean water ranges from 7.5 to 8.4; the pH of the water in a certain area is available in the literature[1].

At frequencies below 200 Hz, the Francois–Garrison equation may be invalid. The results of attenuation measurements at frequencies below 200 Hz were analyzed by Guilysse and Sabathe [15], who argued that the attenuation of sound at these frequencies is caused by the scattering of sound by inhomogeneities of the marine environment. The attenuation coefficient α_4 in this frequency range id independent of frequency, but varies with latitude from 0.004 dB/km in polar waters to 0.0002 dB/km in the tropics. Stojanovic [1] used the value α_4 = 0.003 dB/km. The Francois–Garrison equation is applicable to all ocean conditions in the frequency range from 200 Hz to 1 MHz. Using this equation, the attenuation coefficient can be calculated with an accuracy of 10%. To obtain an expression for the sound attenuation coefficient in the frequency range from 10 Hz to 1 MHz, it is necessary to add the attenuation coefficient α_4 to the Francois–Garrison attenuation coefficient. Further, it is assumed that α_4 = 0.003 dB/km. Therefore, the sound attenuation coefficient at frequency f has the form: $\alpha = \alpha_1 + \alpha_2 + \alpha_3 + \alpha_4$.

To calculate the attenuation coefficient from the Francois–Garrison formula, it is necessary to know the water temperature T, salinity S, pH, and depth z along the entire sound propagation path.

Urick [5] proposed a simpler formula for the sound attenuation coefficient at a water temperature of T = 4°C, which is characteristic of great depths in the deep sea:

$$\alpha_U = \frac{0.11 f^2}{1+f^2} + \frac{44 f^2}{4100+f^2} + 3\cdot 10^{-4} f^2.$$

Here, α_U is the attenuation coefficient, dB/km; and f is frequency, kHz.

The Urick formula is also based on the results of experimental studies, and its components are similar to those of the Francois–Garrison formula. However, Urick [5] provided no information on the accuracy of the approximation of the known expressions for the attenuation coefficient by this formula. Moreover, the frequency range in which this formula is valid was not indicated. It was of interest to compare the Francois–Garrison and Urick attenuation coefficients. Figure 1a illustrates the frequency dependence of the attenuation coefficient calculated by the Francois–Garrison formula. Since, on a logarithmic scale, the Urick curve differs little from the Francois–Garrison curve, the graphs of the Francois–Garrison and Urick attenuation coefficients and their differences were plotted on a linear scale (Fig. 1b).

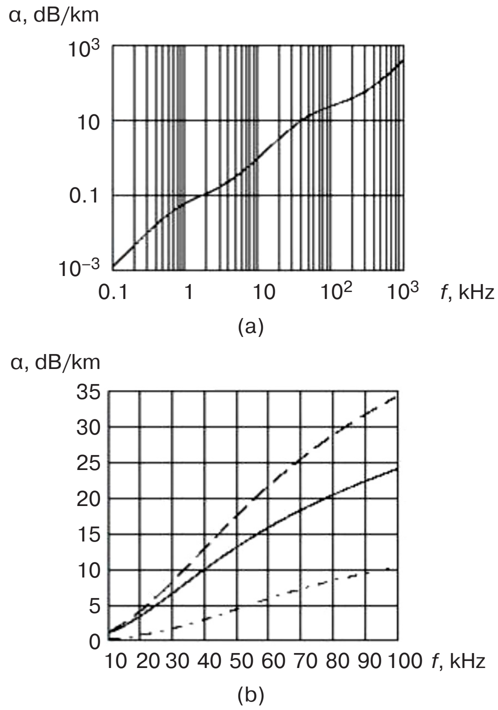

Fig. 1. Attenuation coefficient α versus frequency f in the frequency ranges (a) 0.1–10^3 kHz (Francois–Garrison formula) and (b) 10–100 kHz (the solid and dashed curves were calculated by the Francois–Garrison and Urick formulas, respectively; and the dashed-and-dotted curve represents the difference $\alpha_U(f) - \alpha(f)$)

[1] *Atlas okeanov* (*Atlas of the Oceans*): in 3 v. V. 1. *Tikhii okean* (*Pacific Ocean*). 323 p. V. 2. *Atlanticheskii i Indiiskii okeany* (*Atlantic and Indian Oceans*). 334 p. V. 3. *Severnyi Ledovityi okean* (*Arctic Ocean*). Leningrad: MO USSR; 1974–1980. 188 p. (in Russ.).

Figure 1b shows that the discrepancies between the attenuation coefficients at high frequencies can be significant. The relative error $\delta_\alpha = (\alpha - \alpha_U)/\alpha$ of the approximation of the Francois–Garrison formula by the Urick formula in the frequency range from 0.1 kHz to 1 MHz at a temperature of $T = 4$°C and a seawater salinity of $S = 35$‰ is $\delta_\alpha = -0.26$ at $z = 100$ m and $\delta_\alpha = -0.42$ at $z = 1000$ m. At $S = 30$‰, $|\delta_\alpha|$ increases by half. Such error values can hardly be considered acceptable under these conditions. Therefore, the HACC capacity should be calculated using the Francois–Garrison formula.

Further, let us the express frequency f in hertz. For this purpose, the factor 10^{-3} should be added to the formulas for the coefficients A_1 and A_2; the factor 10^{-6}, to the formula for A_3; and the factor 10^3, to the formulas for the frequencies f_1 and f_2.

2. NOISES OF THE MARINE ENVIRONMENT

The interference considered in this work is the noise that is characteristic of the deep sea. Its main sources in this case are ocean turbulence, long-distance shipping, sea surface waves, and thermal noise generated by the thermal motion of water molecules [5]. At short time intervals and moderate depths, the ambient sea noise can be described by a stationary Gaussian process and characterized by spectral intensity density. Due to the variability of the sources, the ambient noise is characterized by the average spectral intensity density. The graphs of the average spectral intensities of turbulence noise, shipping noise, noise from sea surface waves, and thermal noise in the frequency range 1–10^5 Hz were provided by Urick [5, Fig. 7.5]. Using a piecewise linear approximation of these curves, the following analytical expressions for the spectral noise levels were obtained.

The spectral level of turbulence noise, $N_{tu}(f)$, dB relative to 1 μPa:

$$N_{tu}(f) = (107 - 30\log f)\,[1(f - 1) - 1(f - 50)].$$

The spectral level of shipping noise, $N_{sh}(f)$, dB relative to 1 μPa:

$$\begin{aligned} N_{sh}(f, k) &= (44 + 9k + 20\log f)\,[1(f - 1) - 1(f - 10)] + \\ &+ (64 + 9k)[1(f - 10) - 1(f - 100)] + \\ &(144 + 9k - 40\log f)\,1(f - 100), \end{aligned}$$

where f is frequency, Hz; $1(f)$ is the unit step function; and $k = 0$, 1, and 2 are in the cases of low-, medium-, and high-intensity shipping, respectively.

The spectral level of sea wave noise, $N_w(f)$, dB relative to 1 μPa:

$$\begin{aligned} &N_w(f, b) = \\ &= (N_1 + 20\log f - 46)[1(f - 1) - 1(f - 200)] + \\ &+ N_1[1(f - 200) - 1(f - 1000)] + \\ &+ (N_1 + 60 - 20\log f)\,1(f - 1000), \\ &N_1 = N_1(b) = N_w(f, b)|_{f = 1000\text{ Hz}} = \\ &= 44.9 + 13.4\ln(1 + b). \end{aligned} \tag{4}$$

In the last formulas, b is a numerical quantity, which characterizes the sea state, measured as wave forces, and takes values in the range [0, 6]. Formula (4) was obtained by the least squares approximation of the sequence of the values $N_w(1000, b)$ (b = 0, 0.5, 1, 2, 3, 4, 6) of the family of curves $N_w(f, b)$ presented on a large scale in [16]. The relative approximation error does not exceed 4%.

The spectral level of thermal noise, $N_{th}(f)$, dB relative to 1 μPa:

$$N_{th}(f) = (-75 + 20\log f)\,1(f - 10000). \tag{5}$$

After the determination of the spectral levels of the noises, their spectral intensity densities can be found.

For turbulence noise,

$$\begin{aligned} &J_{tu}(f) = J_0 10^{0.1 N_{tu}(f)} = \\ &= J_0 10^{10.7} f^{-3}[1(f-1) - 1(f-50)],\ \text{W/(cm}^2\cdot\text{Hz)}, \end{aligned}$$

where $J_0 = 0.667 \cdot 10^{-22}$ W/(cm²·Hz) is the reference value of the spectral intensity, which corresponds to a root-mean-square pressure of 1 μPa.

For shipping noise,

$$\begin{aligned} &J_{sh}(f,k) = J_0 10^{0.1 N_{sh}(f)} = \\ &= J_0 10^{4.4 + 0.9k} f^2 [1(f-1) - 1(f-10)] + \\ &+ J_0 10^{6.4 + 0.9k} [1(f-10) - 1(f-100)] + \\ &+ J_0 10^{14.4 + 0.9k} f^{-4} 1(f-100),\ \text{W/(cm}^2\cdot\text{Hz)}. \end{aligned}$$

For noise from sea surface waves,

$$\begin{aligned} &J_w(f,b) = J_0 10^{0.1 N_w(f,b)} = \\ &= J_0 10^{0.1N_1 - 4.6} f^2 [1(f-1) - 1(f-200)] + \\ &+ J_0 10^{0.1N_1} [1(f-200) - 1(f-1000)] + \\ &+ J_0 10^{0.1N_1 + 6} f^{-2} 1(f-1000),\ \text{W/(cm}^2\cdot\text{Hz)}. \end{aligned}$$

For thermal noise,

$$J_{\text{th}}(f) = J_0 10^{0.1 N_{\text{th}}(f)} = \\ = J_0 10^{-7.5} f^2\ 1(f - 10000),\ \text{W/(cm}^2\cdot\text{Hz)}. \quad (6)$$

Expressions (5) and (6) are valid at a water temperature of T = 4°C. At other water temperatures, the spectral density of thermal noise is calculated from the formula

$$J_{\text{th}}(f) = 4\pi k_B \Theta c^{-2} f^2 1(f - 10000),\ \text{W/(cm}^2\cdot\text{Hz)},$$

where k_B = 1.38 · 10^{-23} W/(Hz·K) is the Boltzmann constant and c = 1.5 · 10^{-5} cm/s is the average speed of sound in seawater.

Figure 2 presents the graphs of the spectral intensity density of the total noise of the marine environment,

$$J_n(f) = J_{\text{tu}}(f) + J_{\text{sh}}(f) + J_{\text{w}}(f) + J_{\text{th}}(f),$$

for the case of medium-intensity shipping in various sea states. The solid, dotted, dashed, and dashed-and-dotted lines are plotted at b = 0 (calm sea), 1, 3, and 6, respectively.

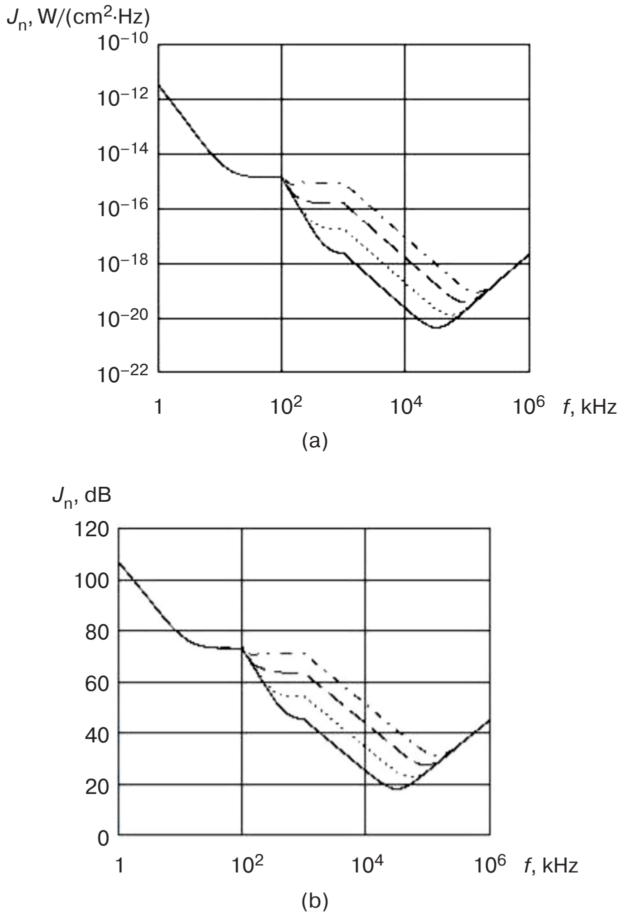

Fig. 2. Spectral intensity density of the total noise of the marine environment in (a) physical units and (b) decibels relative to $J_0 = 0.667 \cdot 10^{-22}$ W/(cm²·Hz)

3. HACC CAPACITY

The HACC under investigation can be represented as a low-pass filter with the complex gain $H(j\omega)$, to the input of which signal (pressure) $p_1(t)$ is applied, and at the output of which signal $p_2(t)$ is received and summed with nonwhite Gaussian sea noise $p_n(t)$. Thus, the process at the HACC has the form $p(t) = p_2(t) + p_n(t)$. Let us consider the signal $p_1(t)$ the realization of a certain constrained-intensity stationary ergodic random process. Let the intensity of the input signal at a distance of 1 m from the source be I_S. Let us determine the HACC capacity under constraints on the bandwidth (by the filter) and on the signal intensity. The capacity of a HACC-like channel under constraints on frequency and average power was found using information theory [17], and it was shown that the capacity is reached if the input signal is a stationary Gaussian process. In terms of this work, the formula for the HACC capacity takes the form

$$C = \int_{f_{\text{lower}}(B)}^{f_{\text{upper}}(B)} \log\left[\frac{H^2(f)B}{J_n(f)}\right] df. \quad (7)$$

Here, $f_{\text{lower}}(B)$ and $f_{\text{upper}}(B)$ is the lower and upper frequencies, respectively, of the bandwidth, for which

$$\frac{J_n(f)}{H^2(f)} \le B, \quad (8)$$

B is the solution of the equation

$$\int_{f_{\text{lower}}(B)}^{f_{\text{upper}}(B)} \left[B - \frac{J_n(f)}{H^2(f)}\right] df = I_S, \quad (9)$$

and $H(f) = |H(j2\pi f)|$ is the the frequency response of the HACC.

The spectral intensity density $J_S(f)$ of the random input signal at which the channel capacity is reached is found by the formula

$$J_S(f) = \begin{cases} B - J_n(f)/H^2(f), & f \in [f_{\text{lower}}(B), f_{\text{upper}}(B)], \\ 0, & f \notin [f_{\text{lower}}(B), f_{\text{upper}}(B)]. \end{cases} \quad (10)$$

Thus, the HACC capacity is determined by two parametric equalities (7) and (9). The parameter is the quantity B, which should satisfy inequality (8). By simultaneously solving equations (7) and (9) under constraint (8), the C and B values can be found, and then from formula (10), the spectrum of the optimal input signal can be determined. This problem can be solved only by numerical methods on a computer.

Figure 3a illustrates the calculated dependence of the capacity $C(R)$ on the communication distance at three values of the input signal intensity for the case of calm sea ($b = 0$) and medium-intensity shipping ($k = 1$).

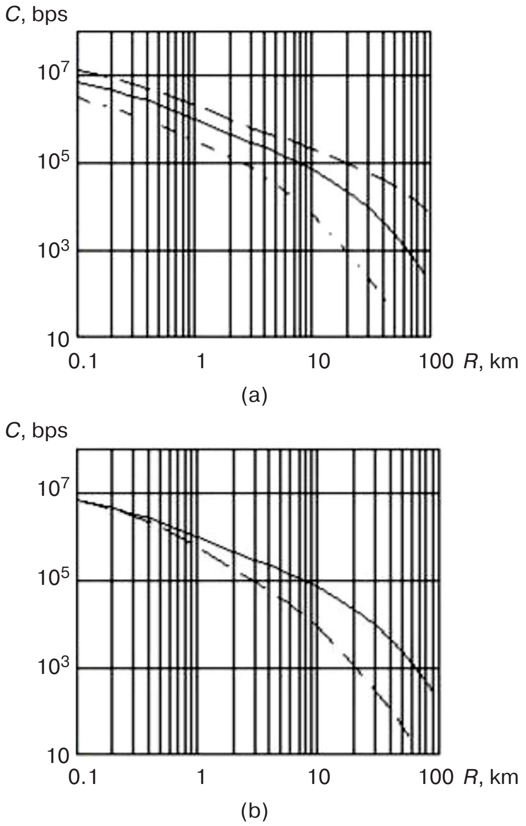

Fig. 3. HACC capacity versus communication distance at $k = 1$: (a) $b = 0$ and $I_S = 10^{-7}$ W/cm^2 (dashed-and-dotted line), $I_S = 10^{-5}$ W/cm^2 (solid line), and $I_S = 10^{-3}$ W/cm^2 (dashed line) and (b) $I_S = 10^{-5}$ W/cm^2 and $b = 3$ (dashed line) and $b = 0$ (solid line)

Figure 3a shows that the capacity decreases with increasing communication distance, and this decrease is the faster, the lower the intensity of the input signal. Figure 3a can be used to estimate the order of magnitude of the capacity under the given communication conditions.

Figure 3b presents the dependences $C(R)$ at $I_S = 10^{-5}$ W/cm^2 and various b. It can be seen that the noise from sea surface waves can significantly decrease the capacity. For example, in calm sea ($b = 0$) at $R = 10$ km, $C = 7 \cdot 10^4$ bps, and if $b = 3$, then $C = 8 \cdot 10^3$ bps.

Calculations showed that, at a constant intensity of the input signal, with increasing distance R, the width of the spectrum of the optimal signal decreases due to an increase in the lower boundary frequency f_{lower} of the spectrum and a decrease in the upper frequency f_{upper}. Figure 4 illustrates the distance dependences of these frequencies at $k = 1$ and $b = 0$.

As an example, Fig. 5 presents two spectra of the optimal signal at constant intensity of the input signal, $k = 1$, $b = 0$, $I_S = 10^{-5}$ W/cm^2, and two values of the distance R.

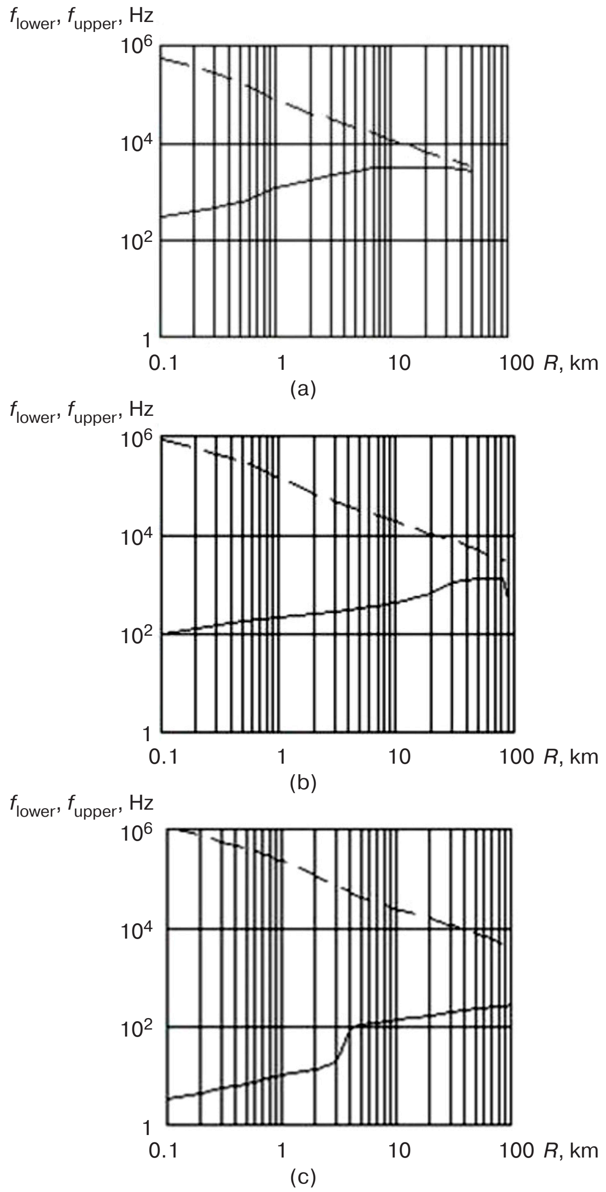

Fig. 4. Dependences of the lower boundary frequency f_{lower} (solid line) and the upper boundary frequency f_{upper} (dashed line) of the optimal spectrum of the input signal on the communication distance at I_S of (a) 10^{-7}, (b) 10^{-5}, and (c) 10^{-3} W/cm^2

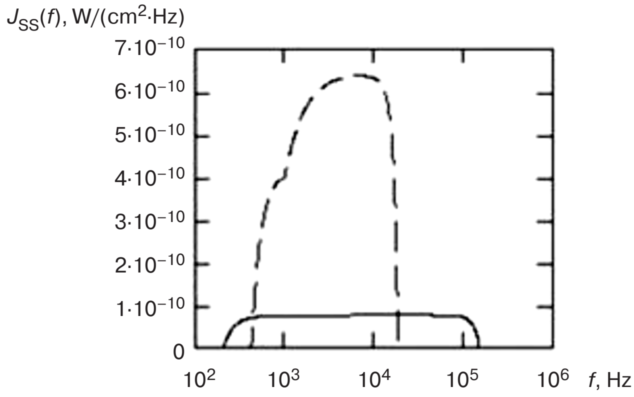

Fig. 5. Optimal spectra of the input signal at various communication distances of $R = 1$ km (solid line) and $R = 10$ km (dashed line)

As can be seen from Fig. 5, with increasing communication distance at constant intensity of the input signal, the optimal spectrum narrows, but its values increase. The spectrum of the optimal input signal is always limited in frequency.

Figure 6 shows the optimal spectra at $k = 1$, $I_S = 10^{-5}$ W/cm^2, and $R = 10$ km in the absence of sea waves ($b = 0$) and in the case of sea waves at $b = 3$. As follows from Fig. 6, the noise from sea waves leads to a decrease in the width of the optimal spectrum, a change in its shape, and an increase in its intensity.

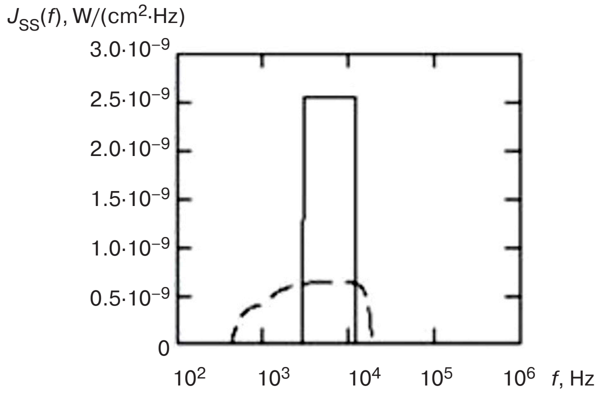

Fig. 6. Optimal spectra of the input signal at various sea wave intensities of $b = 3$ (solid line) an $b = 0$ (dashed line)

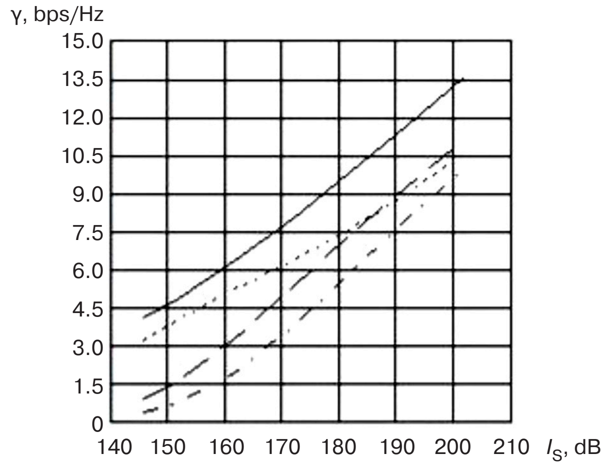

Fig. 7. Bandwidth usage versus input signal intensity at various communication distances of $R = 0.2$ km (solid line), $R = 1$ km (dotted line), $R = 5$ km (dashed line), and $R = 10$ km (dashed-and-dotted line)

As follows from the analysis, the HACC is a constrained-bandwidth channel. Therefore, from a practical point of view, it was of great interest to evaluate the bandwidth usage of the HACC. Figure 7 shows the results of calculations of the dependence of the bandwidth usage $\gamma = C/(f_{upper} - f_{lower})$ on the intensity of the input signal (in decibels relative to 1 μPa) at four communication distances. It can be seen from Fig. 7 that, regardless of the distance, γ increases with increasing input signal intensity. An interesting feature of these dependences is that the curves at $R = 1$ and 5 km intersect at a certain intensity value (in the vicinity of 190 dB). Therefore, there may be cases where the bandwidth usage at a longer distance is greater than that at a shorter distance at the same input signal intensity. From the data in Fig. 7, one can estimate the order of magnitude of the coefficient γ under the specified communication conditions. For example, the maximum value of γ is approximately 13 bps/Hz and occurs at $I_S = 200$ dB and $R = 0.2$ km.

CONCLUSIONS

The main purpose of this work was to determine the capacity of a HACC with constrained average intensity of the transmitted signal. A model of a single-path channel was considered, which is characteristic of the deep sea with the receiver or transmitter placed at a sufficient depth. In this case, the sound propagation to medium distances occurs along "stable" trajectories, which are unaffected by the sea surface and the bottom. Such trajectories exist for vertical and near-vertical (10°–15°) channels.

The comparison of the numerical values of the Francois–Garrison and Urick attenuation coefficients showed that Urick attenuation coefficient can differ markedly from the Francois–Garrison attenuation coefficient. Moreover, the Francois–Garrison attenuation coefficient takes into account the dependence of the sound attenuation on the seawater parameters. Therefore, in this work, the Francois–Garrison attenuation coefficient was used. Using it, the complex gain, the frequency response, and the phase response of the HACC were obtained.

A new expression was derived for the spectral level of sea noise caused by sea surface waves. The expression for the spectral density of the sea noise intensity used to calculate the channel capacity was obtained by subjecting Urick's curves of the spectral levels of noises from turbulence, shipping, sea waves, and thermal noise to a piecewise linear approximation. The Francois–Garrison attenuation coefficient was used to relate the HACC capacity with the parameters of the marine environment: temperature, salinity, and pH of the study area.

The capacity was calculated for the cases of medium-intensity shipping in calm sea and in Beaufort force 3 waves. It was found that HACC capacity is significantly reduced by noise from sea surface waves. The dependencies of channel capacity on communication distance and the intensity of the transmitted signal were calculated. At a given intensity of the input signal, channel capacity was observed to significantly decrease with increasing distance.

The lower and upper boundary frequencies of the optimal spectrum of the input signal were determined along with the optimal spectrum itself. It was shown that, with increasing communication distance, the width of the optimal spectrum also decreases. A significant effect of noise from sea waves on the shape of the optimal spectrum and the values of its boundary frequencies can be noted.

The dependence of bandwidth usage on the intensity of the input signal at various communication distances was characterized. Under some conditions, there may be cases where bandwidth usage increases with increasing distance at a given input signal intensity.

REFERENCES

1. Stojanovic M. On the relationship between capacity and distance in an underwater acoustic communication channel. *ACM SIGMOBILE Mobile Computing and Communications Review.* 2007;11(4):34–43. https://doi.org/10.1145/1347364.1347373
2. Lucani D.E., Stojanovic M., Medard M. On the relationship between transmission power and capacity of an underwater acoustic communication channel. In: *Proceedings of OCEANS Conference*. 2008. 6 p. https://doi.org/10.1109/OCEANSKOBE.2008.4531073
3. Stojanovic M., Preisig J. Underwater acoustic communication channels: propagation models and statistical characterization. *IEEE Communications Magazine*. 2009;47(1):84–89.
4. Matarneh A.M. Thorough investigation of BER simulation of DPSK in underwater acoustic channel. *JJEE*. 2016;2(2):160–171.
5. Urik R.J. *Osnovy gidroakustiki* (*Principles of Underwater Sound*). Leningrad: Sudostroenie; 1978. 445 p. (in Russ.).
[Urik R.J. *Principles of Underwater Sound*. NY: McGraw-Hill, Book Company; 1975. 445 p.]
6. Coates R. *Underwater Acoustic Systems*. New York: Wiley; 1990. 188 p.
7. Sivers M.A., Basov V.V. The use of MIMO-OFDM technology in systems of the hydrolocation, hydroacoustic communication, navigation and management. In: *Wave Electronics and Infocommunication Systems*: *Proceedings of the 23rd International Scientific Conference*. In 2 v. V. 2. St. Petersburg; 2020. P. 177–183 (in Russ.).
8. Eroshenko S.V., Krants V.Z., Sechin V.V. On the use of parallel channels to increase information rate in hydroacoustic communication system with compound signals. *Gidroakustika = Hydroacoustics.* 2020;42(2): 21–28 (in Russ.).
9. Rodionov A.Yu., Unru P.P., Kulik S.Yu., Golov A.A. Application of multi-frequency signals with constant envelope in underwater communication systems. *Podvodnye issledovaniya i robototekhnika = Underwater Investigations and Robotics*. 2019;3(29):30–38 (in Russ.). https://doi.org/10.25808/24094609.2019.29.3.004
10. Klei K., Medvin G. *Akusticheskaya okeanografiya* (*Acoustical Oceanography*): trans. from Eng. Moscow: Mir; 1980. 580 p. (in Russ.).
[Clay C.S., Medwin H. *Acoustical Oceanography*. New York: Wiley; 1977. 544 p.]
11. Brekhovskikh L.M., Lysanov Yu.P. *Teoreticheskie osnovy akustiki okeana* (*Theoretical Foundations of Ocean Acoustics*). Leningrad: Gidrometeoizdat; 1982. 264 p. (in Russ.).
12. Andreeva I.B. *Fizicheskie osnovy rasprostraneniya zvuka v okeane* (*Physical Foundations of Sound Propagation in the Ocean*). Leningrad: Gidrometeoizdat; 1975. 190 p. (in Russ.).

СПИСОК ЛИТЕРАТУРЫ

1. Stojanovic M. On the relationship between capacity and distance in an underwater acoustic communication channel. *ACM SIGMOBILE Mobile Computing and Communications Review.* 2007;11(4):34–43. https://doi.org/10.1145/1347364.1347373
2. Lucani D.E., Stojanovic M., Medard M. On the relationship between transmission power and capacity of an underwater acoustic communication channel. In: *Proceedings of OCEANS Conference*. 2008. 6 p. https://doi.org/10.1109/OCEANSKOBE.2008.4531073
3. Stojanovic M., Preisig J. Underwater acoustic communication channels: propagation models and statistical characterization. *IEEE Communications Magazine*. 2009;47(1):84–89.
4. Matarneh A.M. Thorough investigation of BER simulation of DPSK in underwater acoustic channel. *JJEE*. 2016;2(2):160–171.
5. Урик Р.Дж. *Основы гидроакустики*: пер. с англ. Л.: Судостроение; 1978. 445 с.
6. Coates R. *Underwater Acoustic Systems*. New York: Wiley; 1990. 188 p.
7. Сиверс М.А., Басов В.В. Использование технологии MIMO-OFDM в системах гидролокации, гидроакустической связи, навигации и управления. В сб.: *Волновая электроника и инфокоммуникационные системы: Материалы XXIII международной научной конференции*: в 2 ч. Часть 2. Санкт-Петербург; 2020. С. 177–183.
8. Ерошенко С.В., Кранц В.З., Сечин В.В. Об использовании параллельных каналов для повышения скорости передачи информации в системе гидроакустической связи со сложными сигналами. *Гидроакустика.* 2020;42(2):23–28.
9. Родионов А.Ю., Унру П.П., Кулик С.Ю., Голов А.А. Оценки применения многочастотных сигналов с постоянной огибающей в гидроакустических системах связи. *Подводные исследования и робототехника*. 2019;3(29):30–38. https://doi.org/10.25808/24094609.2019.29.3.004
10. Клей К., Медвин Г. *Акустическая океанография*: пер. с англ. М.: Мир; 1980. 580 с.
11. Бреховских Л.М., Лысанов Ю.П. *Теоретические основы акустики океана*. Л.: Гидрометеоиздат; 1982. 264 с.
12. Андреева И.Б. *Физические основы распространения звука в океане*. Л.: Гидрометеоиздат; 1975. 190 с.
13. Francois R.E., Garrison G.R. Sound absorption based on ocean measurements: Part I: Pure water and magnesium sulfate contributions. *J. Acoust. Soc. Am*. 1982;72(3): 896–907. https://doi.org/10.1121/1.388170
14. Francois R.E., Garrison G.R. Sound absorption based on ocean measurements: Part II: Boric acid contribution and equation for total absorption. *J. Acoust. Soc. Am.* 1982;72(6):1879–1890. https://doi.org/10.1121/1.388673

13. Francois R.E., Garrison G.R. Sound absorption based on ocean measurements: Part I: Pure water and magnesium sulfate contributions. *J. Acoust. Soc. Am*. 1982;72(3): 896–907. https://doi.org/10.1121/1.388170
14. Francois R.E., Garrison G.R. Sound absorption based on ocean measurements: Part II: Boric acid contribution and equation for total absorption. *J. Acoust. Soc. Am.* 1982;72(6):1879–1890. https://doi.org/10.1121/1.388673
15. Kibblevhite A.C., Hampton L.D. A review of deep ocean sound attenuation data at very low frequencies. *J. Acoust. Soc. Am*. 1980;67(1):147–157. https://doi.org/10.1121/1.384473
16. Guies L., Sabate P. *Osnovy akustiki morya* (*Fundamentals of acoustics of the sea*): trans. from Franc. Leningrad: Gidrometeoizdat; 1967. 212 p. (in Russ.).
17. Galager R. *Teoriya informatsii i nadezhnaya svyaz'* (*Information Theory and Reliable Communication*): trans. from Eng. Moscow: Sovetskoe Radio; 1974. 720 p. (in Russ.).
[Gallager R.G. *Information Theory and Reliable Communication*. NY: J. Wiley; 1968. 603 p.]

15. Kibblevhite A.C., Hampton L.D. A review of deep ocean sound attenuation data at very low frequencies. *J. Acoust. Soc. Am*. 1980;67(1):147–157. https://doi.org/10.1121/1.384473
16. Гийес Л., Сабате П. *Основы акустики моря*: пер. с фр. Л.: Гидрометеоиздат; 1967. 212 с.
17. Галагер Р. *Теория информации и надежная связь*: пер. с англ. М.: Сов. Радио; 1974. 720 с.

About the author

Valery E. Denisov, Senior Lecturer, Department of Radio Wave Processes and Technologies, Institute of Radio Electronics and Informatics, MIREA – Russian Technological University (78 Vernadskogo pr., Moscow, 119454 Russia). E-mail: denisov@mirea.ru. RCSI SPIN-code 1190-9380, https://orcid.org/0000-0002-5824-8741

Об авторе

Денисов Валерий Евгеньевич, старший преподаватель кафедры радиоволновых процессов и технологий Института радиоэлектроники и информатики ФБГОУ ВО «МИРЭА – Российский технологический университет» (119454, Россия, Москва, пр–т Вернадского, д. 78). E-mail: denisov@mirea.ru. SPIN-код РИНЦ 1190-9380, https://orcid.org/0000-0002-5824-8741

Translated from Russian into English by Vladislav V. Glyanchenko
Edited for English language and spelling by Thomas A. Beavitt